

IDŐJÁRÁS

*Quarterly Journal of the Hungarian Meteorological Service
Vol. 127, No. 1, January – March, 2023, pp. 1–22*

Assessment of WRF planetary boundary layer schemes in the simulation of fog events over Hungary

Jeevan Kumar B * and **Gabriella Schmeller**

*University of Pécs, Faculty of Science
Ifjúság str 6, H-7624 Pécs, Hungary.*

**Corresponding author E-mail: jeevan@gamma.ttk.pte.hu*

(Manuscript received in final form April 19, 2022)

Abstract—Accurate depiction of meteorological conditions, especially within the planetary boundary layer (PBL), is essential for fog forecasting. This study examines the sensitivity of the performance of the Weather Research and Forecast (WRF) model to the use of four different PBL schemes [Yonsei University (YSU), asymmetric convective model version 2 (ACM2), quasnormal scale elimination (QNSE), and Mellor-Yamada-Nakanishi-Niino version 3.0 (MYNN3)]. For this case study we have taken the fog event occurred in November 23–24, 2020. Surface observed temperature and relative humidity, furthermore, sounding data are compared with the output of the 36 hours, high-resolution weather forecast. The horizontal extension of the simulated fog is compared with satellite observations. The visibility is calculated from the prognostic variables of drop number concentration and mixing ratio. The simulated visibility and fog duration are validated by the visibility and fog duration evaluated by ceilometer observations. Validation of thermodynamical values such as 2-m temperature and relative humidity reveals, that during most of the simulation time, the bias is significant between the simulated and observed data. Results show that the PBL parameterization scheme significantly impacts fog microphysics also. The QNSE scheme results in unrealistic early formation of the fog, and too large liquid water content. YSU and ACM2 simulated the duration of fog to be rather short comparing with the other two PBL schemes. The best fitting with observed data is found in the case of MYNN3 PBL schemes.

Key-words: fog, WRF, planetary boundary layer, Goddard Chemistry Aerosol Radiation and Transport (GOCART)

1. Introduction

Fog is a boundary layer weather phenomenon with tiny droplets of water or ice crystals formed near-surface in a diameter range of $\sim 2\text{--}30\ \mu\text{m}$ reducing the horizontal visibility in the atmosphere near the surface less than 1 km (*Gulpepe et al.*, 2007). Fog is one of the significant weather hazards that affects aviation, road transportation, economy, and public health worldwide. However, very few studies were carried out to understand the fog characteristics over Hungary. *Cséplő et al.*, 2019 investigated fog climatology and long-term trends in Hungary.

Forecasting of fog remains a challenge because of diversity of processes including the drop formation on submicron size aerosol particles, turbulence, radiation, and soil effects. Although researchers carried out multiple field experiments and contributed progress in understanding fog processes, uncertainties remain in the physical mechanisms driving the fog variability. Noteworthy studies include campaigns in the Po Valley in Italy (*Fuzzi et al.*, 1998), Paris fog in France (*Haeffelin et al.*, 2010), and winter fog experiments over New Delhi (*Ghude et al.*, 2017).

However, numerical models were also used to study fog to fill the inconsistencies between observational challenges. Conventional empirical models/techniques are not uncommonly accurate in the case of fog forecasting, and mesoscale weather prediction models could not yet adequately be developed for predicting fog and visibility conditions near the surface. There are many models available to simulate the weather, such as the U.S. Rapid Update Cycle (RUC) model (*Benjamin et al.*, 2004), the Weather Research and Forecasting (WRF) model (*Skamarock et al.*, 2008), the Consortium for Small Scale Modeling (COSMO) (*Rockel et al.*, 2008), the Japan Meteorological Agency Non-Hydrostatic Model (JMA-NHM) (*Saito et al.*, 2006), and the Canadian Mesoscale Compressible Community (MC2) model (*Benoit et al.*, 1997). Among all models, WRF is widely used to forecast the weather and also for research purposes (e.g., *Geresdi et al.*, 2020; *Horváth et al.*, 2007; *Sarkadi et al.*, 2016).

The WRF model has a broad spectrum of physical parameterizations representing the sub-scale cumulus formation, cloud microphysics, planetary boundary layer (PBL), atmospheric radiation, and land surface processes that account for the interaction between the atmosphere and the Earth's surface. The proposed parameterization options in WRF range from basic to more subtle and computationally costly systems that are revised permanently with newly updated/developed model versions. Depending on the model domain, spatial resolution, location, and application, researchers are published different simulation performances using various combinations of physical schemes to simulate atmospheric processes (e.g., *Lábó and Geresdi*, 2016; *Thériault et al.*, 2015). A wide range of WRF communities from all over the world made several sensitivity tests to perform weather simulations according to their requirements

and areas of interest (*Chaouch et al., 2017; Horváth et al., 2009; Pithani et al., 2019a, 2018a*).

Microphysical processes play a controlling role in the evolution of fog. Cloud microphysics is affected by aerosol particles through initiation of the liquid drop and ice formation. Increase of water-soluble aerosol concentration generally leads to increase of droplet concentration impacting both the lifetime and the efficiency of the precipitation formation (*Twomey, 1984*). *Thompson and Eidhammer (2014a)* introduced a new updated WRF microphysics scheme which allowed us to consider the temporal and spatial variability of aerosol particles evaluated by the Goddard Chemistry Aerosol Radiation and Transport (GOCART) model (*Chin et al., 2002; Ginoux et al., 2001*). The output of GOCART model includes mass mixing ratio of sulfates, sea salts, organic carbon, dust, and black carbon data.

The processes occur in the planetary boundary layer (hereafter PBL) significantly impacting the characteristics of the fog (e.g., duration, visibility). Our understanding about the PBL processes and their effect on the fog are still incomplete. In this study, sensitivity test has been performed to compare the results of using different PBL parameterization schemes.

2. Data and methods

2.1. Observations

For this modeling experiment we have taken the fog event occurred in the morning of November 24, 2020 as a case study. *Fig. 1* shows the EUMETSAT satellite image of fog covered large part of Hungary at 07:10 on November 24, 2020 local time. At this time, fog covered the eastern and northwestern parts of Hungary.

The time evolution of back scatter profiles observed by ceilometer over Pécs and Szeged are depicted in *Fig. 2*. *Fig. 2* shows that while at Szeged fog existed during morning, and before noon fog lifted up due to solar radiation, at Pécs fog did not formed, only low level cloud was detected at late afternoon. The vertical extension of the fog changed between 80 and 100 m. Satellite image also shows the presence and absence of fog at the observational sites of Pécs and Szeged (*Fig. 1*).

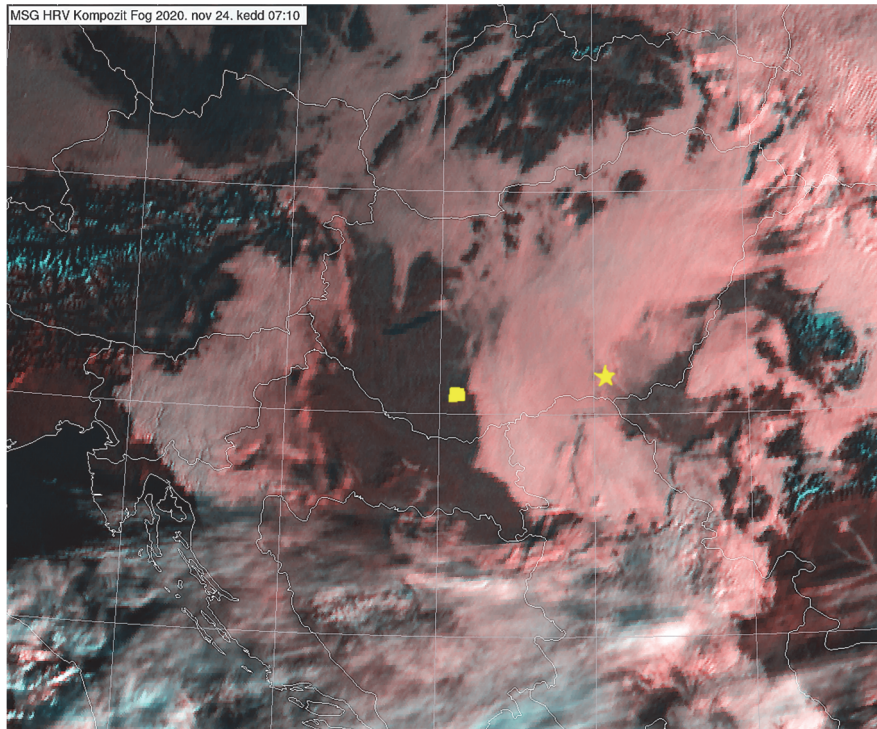


Fig. 1. Satellite image of fog at 07:10 CET (06:10 UTC) on Nov 24, 2020. [Square and star symbols shows Péc and Szeged meteorological stations, respectively.]

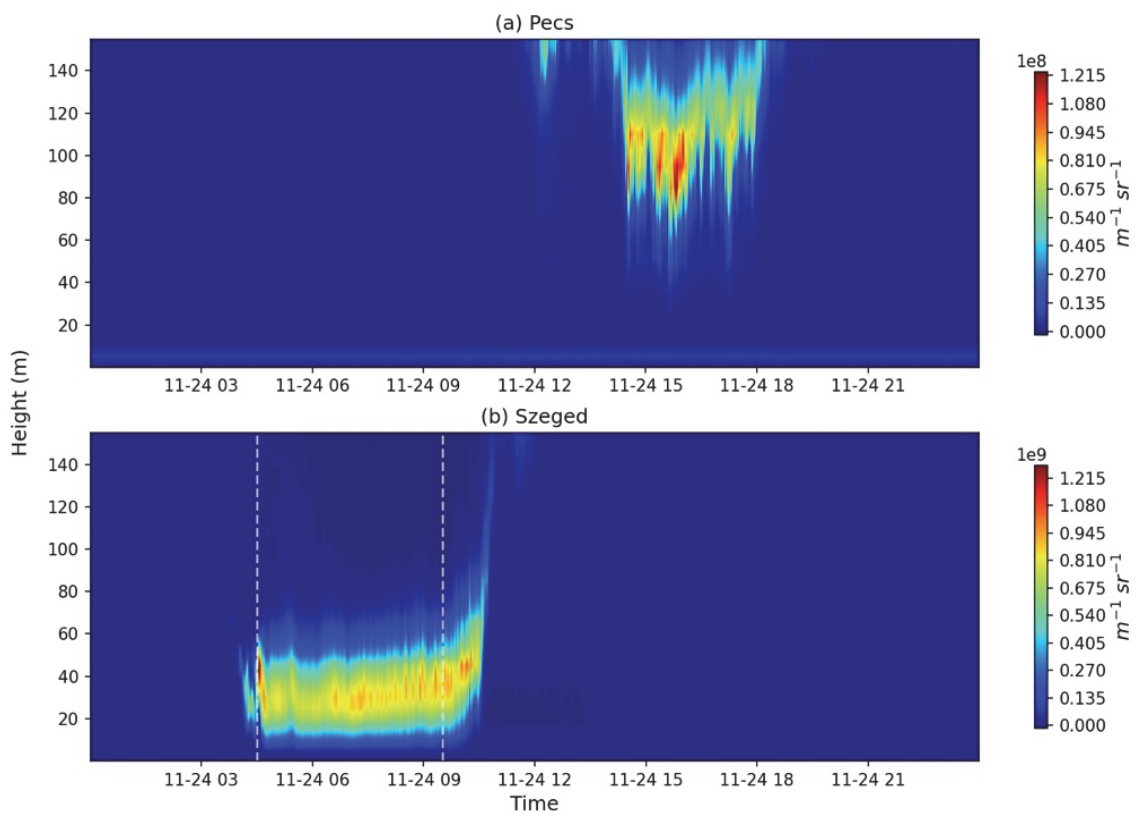


Fig. 2. Back scatter data from Péc (a) and Szeged (b) on Nov 24, 2020. Time is depicted as month-day hour (in CET).

Black solid lines in *Fig. 3* denotes the visibility calculated from ceilometer backscattered data over Szeged. Colored lines depict the time evolution of simulated visibility (at the first model level) using different PBL schemes.

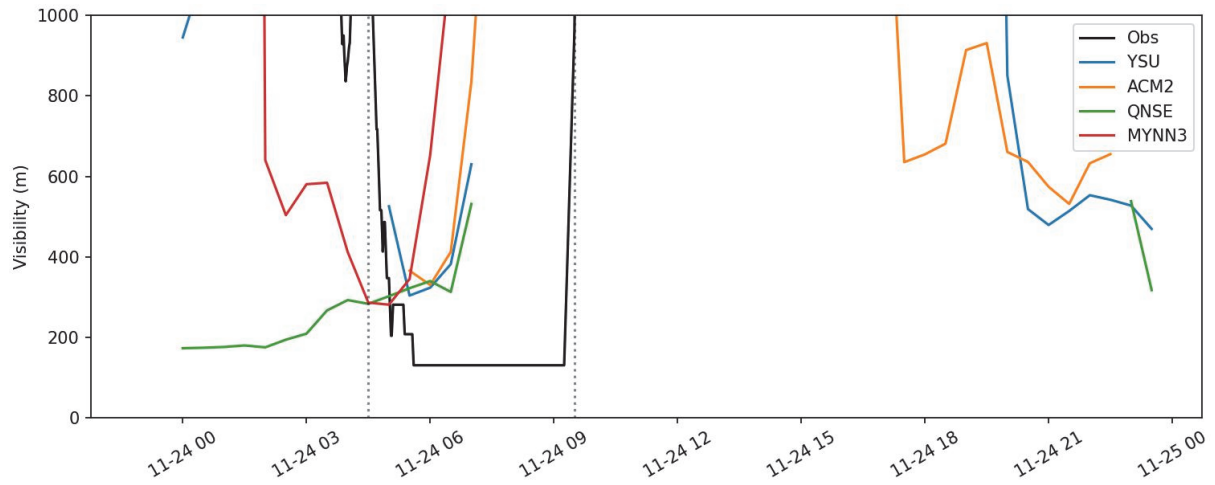


Fig. 3. Calculated visibility data from ceilometer backscattered data and model simulated visibility over Szeged. Note: data are plotted only at Szeged, because fog was not detected at Pécs. Time is depicted as month-day hour (in CET).

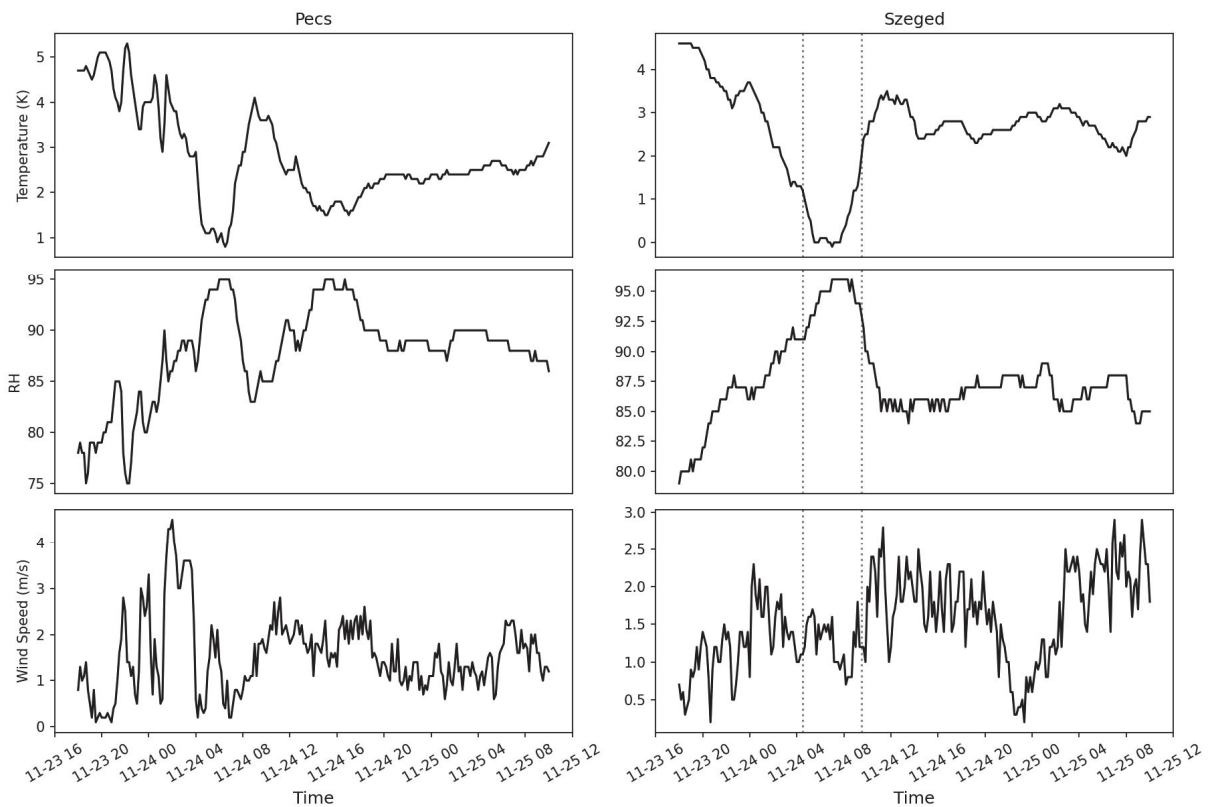


Fig. 4. Time evolution of the surface meteorological parameters (temperature and relative humidity 2 m above the surface, and wind speed at the first model level) over Pécs and Szeged. Vertical, dotted lines for Szeged column indicate the detected fog period. Time is depicted as month-day hour (in CET).

Fig. 4 shows the diurnal cycle of temperature, relative humidity and wind speed at Pécs and Szeged. Calm winds, decreasing temperature, and increasing relative humidity are showing favorable conditions for fog formation both at Pécs and Szeged. Due to measurement errors in the instruments, the relative humidity sensors measure up to 95%, and they usually do not reach 100% (*Gultepe, 2019, 2007*). However, fog was detected only over Szeged, where visibility decreased sharply early morning and became as low as 200 m at 04:30 UTC, indicating the formation of fog. The visibility increased sharply shortly at about 09:30 UTC in response to increasing temperature (*Fig. 3*).

2.2. Model description

Several sensitivity experiments have been accomplished to study how the accuracy of fog forecast depends on planetary boundary layer (PBL) schemes implemented in the WRF Advanced Research Core (ARW, V4.3). The horizontal extension of the model domain is $800 \text{ km} \times 740 \text{ km}$ with horizontal spatial resolution of 2 km. The domain covers the whole territory of Hungary and some part of Hungary's neighbor countries Austria, Croatia, Bosnia, Serbia, Romania, Ukraine, and Slovakia. We use Lambert coordinate configuration with center at 47°N and 19°W to define the domain, and 61 vertical levels (18 levels below 1000 m and 8 levels below 100 m). The large vertical spatial resolution under 100 m allows to properly simulate the vertical structure of the fog and to resolve the inversion layer formed at the top of the fog.

Meteorological initial and boundary conditions are provided by reanalysis products of the European Centre for Medium-Range Weather Forecasting (ECMWF). ERA5 data are operational global analyses available on $0.25^\circ \times 0.25^\circ$ grids with 1 h temporal resolution. For the mesoscale simulations, the geographical data for the land-use and topography are obtained from the standard U.S. Geological Survey dataset (

Fig. 5). Initial conditions at 18:00 UTC on November 23, 2020 are selected for simulation of the fog.

The following parameterization schemes are set to simulate the different physical processes: (i) the rapid radiative transfer model (RRMTG) for both longwave radiation and shortwave radiation (*Iacono et al., 2008*); (ii) the Thompson aerosol aware two-moment bulk scheme for microphysics (*Thompson and Eidhammer, 2014b*), (iii) Noah land surface scheme to simulate the impact of the soil and land use (*Chen and Dudhia, 2001*). The advantage of the Thompson scheme (*Thompson and Eidhammer (2014b)*), compared with other bulk microphysics schemes, is that it able to take into consideration the spatial and temporal variability of the concentration of aerosol particles impacting both the drop and ice formation. This microphysics scheme allows us to evaluate not only the liquid water content (hereafter LWC), but the number concentration of liquid drops explicitly as well. The calculation of prognostic variable of number

concentration of liquid drops not only results in more reliable forecast for the fog formation, but also improve the accuracy of the evaluation of the visibility.

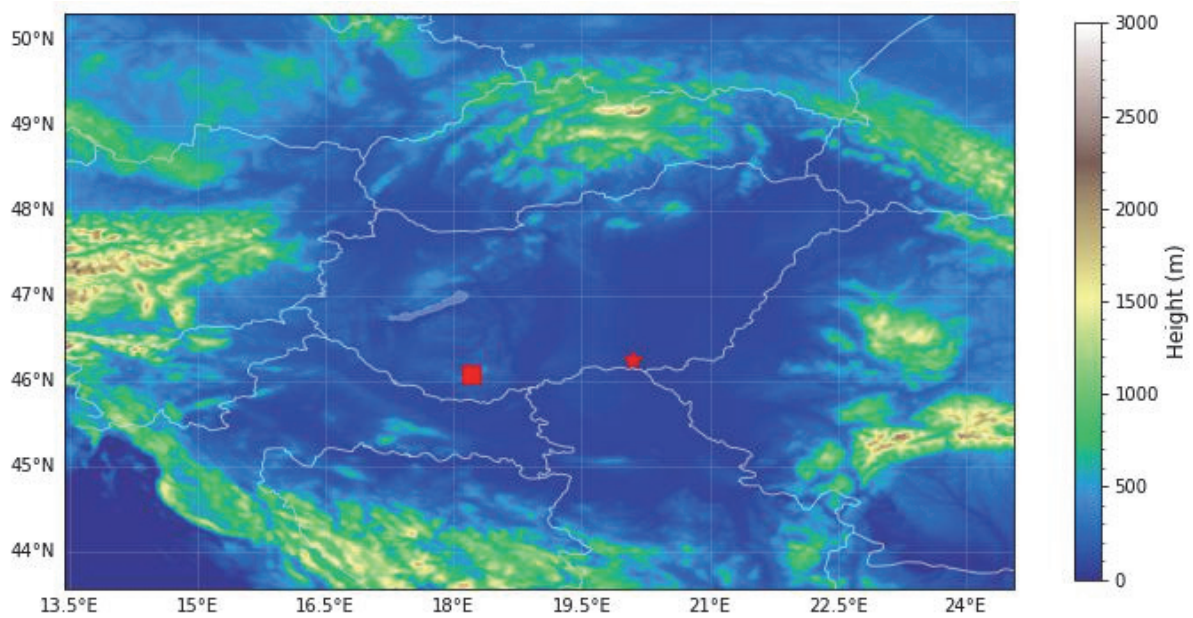


Fig. 5. Topography of WRF model domain with observational sites (square indicates Pécs and star indicates Szeged).

The PBL schemes and surface layer (SFC) formulations are set to be different in each experiment. PBL schemes parameterize turbulent vertical fluxes of heat, momentum, and components like moisture in the PBL. Because some of PBL schemes are suggested tightly coupled to particular surface layer schemes in WRF, it is not possible to have a common surface layer scheme for all experiments. In this case study, we utilized four PBL schemes, MYNN3.0 (Nakanishi and Niino, 2006), YSU (Hong et al., 2006), QNSE (Sukoriansky et al., 2005), and ACM2 (Pleim, 2007). The considered four PBL schemes and the coupled surface schemes are given in Table 1. Cohen et al., 2015 asserted that MYNN3.0 was reasonably good at the simulation of radiation fog development. The YSU scheme enhances mixing in the stable boundary layer by increasing the critical bulk Richardson number from 0 to 0.25 over land (Chen et al., 2020). The ACM2 scheme (Pleim, 2007) was elaborated to improve the shape of vertical profiles of temperature and dew point temperature near the surface. Both nonlocal schemes (YSU & ACM2) may result in strong vertical mixing, sometimes drier and warmer daytime PBLs. In the local scheme, the eddy diffusivity is determined independently at each point grid point, based on local vertical gradients of wind and potential temperature. The nonlocal scheme determines an eddy diffusivity profile based on a diagnosed boundary layer height and a turbulent vertical scale (Mihailovic, 2006).

Table 1. WRF model configuration and initial conditions

Test	Model specification
Initial boundary conditions	WRF-ECMWF
Model domain and resolution	400 × 370 grid points (2 km)
Land use and land category	USGS
Vertical resolution	61 vertical levels (18 levels below 1000 m and 8 levels below 100 m)
Radiation scheme (LW & SW)	RRTMG
Microphysics scheme	Aerosol-aware Thompson scheme
Land surface physics	Noah-mp land surface model
PBL & Surface layer physics	<ol style="list-style-type: none"> 1. YSU and MM5 (Monin-Obukhov scheme) 2. Eddy-diffusivity mass flux (QNSE) and QNSE. 3. MYNN3 and MYNN 4. ACM2 and Pleim-Xiu
Spin up	4 hours (model initialized at 18:00 hour UTC)

Detailed descriptions of PBL schemes are given in the following sections.

2.2.1. YSU

The YSU scheme is a first-order nonlocal closure scheme (*Hong et al., 2006*). It utilizes a turbulence diffusion equation to derive prognostic flux variables within the mixed layer based on an eddy diffusivity coefficient and a counter gradient correction term. The counter gradient correction term accounts for the contribution of the large-scale eddies to the total flux. In the YSU scheme, entrainment is explicitly parameterized through an additional term in the turbulence diffusion equation. The scheme calculates the PBL height by considering bulk Richardson number (Ri_B) values calculated from the surface. Also, the YSU scheme is more effective at representing deep vertical mixing in buoyancy-driven PBLs with shallower mixing in strong-wind regimes (*Hong et al., 2006*). Also, it has been found that the depth of the PBL is overestimated for springtime deep convective environments, resulting in too much dry air near the surface and underestimation of convective available potential energy in the mixed layer.

2.2.2. ACM2

The asymmetrical convective model version 2 (ACM2) scheme is a first-order closure scheme (Pleim, 2007). It is a hybrid local - nonlocal closure scheme. In the ACM2 scheme, the upward fluxes from the surface interact with each layer to account for convective plumes emanating from the surface. On the other hand, the downward fluxes only interact between the adjacent layers. Eddy diffusion is treated locally for both upward and downward fluxes. The scheme utilizes only the local mixing for upward, and downward mixing for stable/neutral flow regimes. In ACM2, the calculation of the PBL height is based on the bulk Richardson number (Ri_B). It is determined as the height where the Ri_B calculated above the neutral buoyancy level is greater than a critical Ri_B value of 0.25. Pleim (2007a) indicated that the profile of potential temperature and velocity through the PBL are depicted with greater accuracy when both local and nonlocal viewpoints are considered regarding vertical mixing (ACM2); Pleim (2007) further validated the use of the ACM2 scheme owing to its support of PBL heights similar to those based on afternoon wind profiler data from radar. However, Coniglio (2012) reported that the scheme produces PBLs were too deep in the evening compared to sounding data.

2.2.3. QNSE

The quasi-normal scale elimination (QNSE) scheme is a 1.5-order local closure scheme (Sukoriansky *et al.*, 2005). It is a spectral model designed for turbulent flows characterized by stable stratification. The scheme involves a quasi-Gaussian mapping of the velocity and temperature fields to account for wave phenomena in stable boundary layers. A stratification scale-dependent elimination algorithm explicitly accounts for the combined effect of turbulence and internal waves. As stratification increases, energy is accumulated in the horizontal flow components at the expense of the energy for the vertical flow components. The scheme calculates the PBL height as the height at which the TKE profile decreases to a value of $0.01 \text{ m}^2 \text{ s}^{-2}$. The scheme provides realistic depiction of potential temperature profiles, PBL height, and kinematic profiles based on observational data and corresponding large eddy simulations (Cohen *et al.*, 2015) for its designed environment (stable conditions). However, in the case of the less-stable PBL, QNSE depicts too cool, moist, and shallow PBL in the case of springtime convective environments.

2.2.4. MYNN

The Mellor-Yamada-Nakanishi-Niino Level 3 (MYNN) scheme is a second-order local closure scheme (Nakanishi and Niino, 2006). In the MYNN3 scheme, equations for stability and mixing length are based on the results of large eddy simulations rather than on observations. Compared with older versions (MJY,

MYNN2.5), MYNN3 more accurately portrays deeper mixed layers and reasonably depicts statically stable boundary layer simulations supporting radiation fog development (Nakanishi and Niino, 2006). However, just like the other local closure schemes, it still may not fully account for deeper vertical mixing associated with larger eddies and associated counter gradient flux correction terms (Cohen *et al.*, 2015).

The above sections reveal the major advantages and disadvantages of four different PBL schemes. Further detailed information about all applied PBL schemes can be found in the following papers: Chaouch *et al.*, 2017; Cohen *et al.*, 2015; García-Díez *et al.*, 2013; Hu *et al.*, 2010; Pithani *et al.*, 2019a.

3. Results

3.1. Analysis of the model data

Model (1st level) corresponding grid point 2 m temperature (hereafter T2) is evaluated for comparison with observation data measured at Pécs and Szeged locations (Fig. 6).

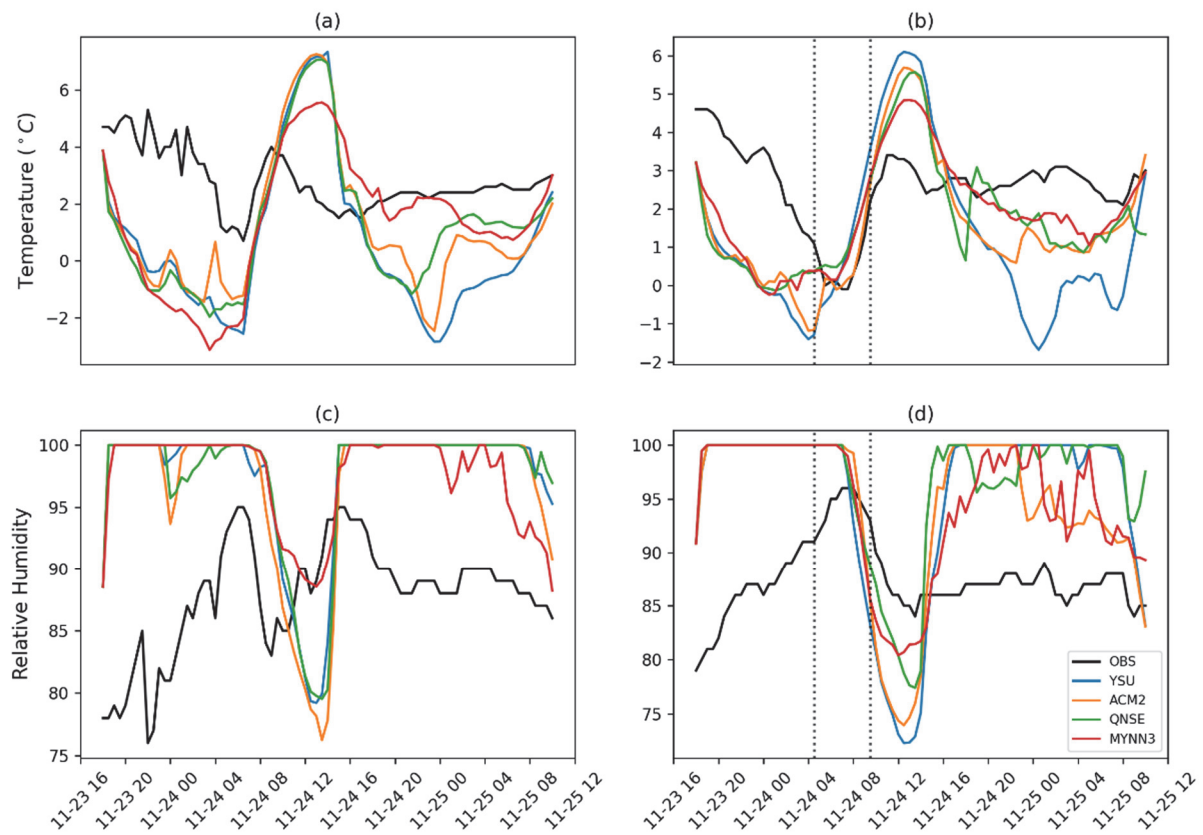


Fig. 6. Time evolution of observed and simulated 2 m temperature and relative humidity weather stations of Pécs and Szeged. Black lines denote the observed values, colored lines correspond to the different PBL schemes (see the legend in (d)). Time is depicted as month-day hour (in CET).

It was found, that the simulated T2 suffers from substantial warm and cold bias during most of the simulated time period (approximately 3–5 °C; *Fig. 6*) independently of the applied PBL scheme. However, fog event was noticed in Szeged on November 24, 2020 between 04:30 – 09:30 UTC, and no fog event was noticed at the Pécs weather station (*Fig. 2*). Comparison of the observed and simulated time profiles of temperature (*Figs. 6a* and *6c*) shows that the temperature was underestimated during middle nights by numerical simulation (independently of the applied PBL schemes), and it was overestimated during afternoon time at both Pécs and Szeged locations. However, all PBL schemes simulated well the change of the temperature during morning time, and the MYNN3 scheme was slightly better than others throughout the simulation period. While the calculated relative humidity was near to 100% during almost the whole simulated time period, the observed RH never reached this maximum value (note the observation error about RH). However, the decrease of simulated RH starts earlier, and it is steeper than the observed one.

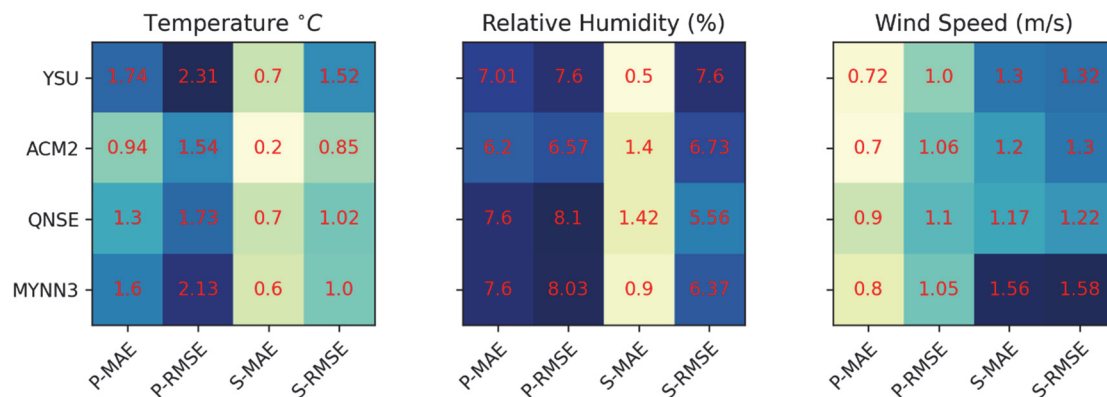


Fig. 7. Heat map of error statistics for the PBL sensitivity simulations over Pécs and Szeged for the observed fog period (see the vertical dashed line in *Fig. 6*). P-MAE indicates the mean absolute error over Pécs and P-RMSE indicates root mean square error over Pécs. S-MAE indicates the mean absolute error over Szeged and P-RMSE indicates root mean square error over Szeged.

Fig. 7 shows the heatmap of calculated error statistics for the PBL sensitivities for the simulation of the fog period at Szeged and Pécs to reveal the performance of the model with each PBL and to identify the better performing schemes. *Fig. 7* gives the mean absolute error (MAE) and root mean square error (RMSE) statistics for temperature, wind speed, and relative humidity at Pécs and Szeged. ACM2 PBL scheme produced comparatively better MAE and RMSE values for the temperature at both locations (Pécs: 0.94 and 1.54 °C, Szeged: 0.2 and 0.85 °C) during the fog period. YSU scheme shows the largest of temperature

bias, and it results in the largest mean absolute error and root mean square error. In the case of relative humidity, ACM2 gave better result only with MAE and RMSE over Pécs, but YSU scheme has low MAE and QNSE has low RMSE value over Szeged. For wind speed, ACM2 has low MAE, and MYNN3 has low RMSE values over Pécs, and QNSE has low MAE and RMSE values in Szeged. The best fitting between the observed and simulated temperature and relative humidity occurs in the case of MYNN3 scheme.

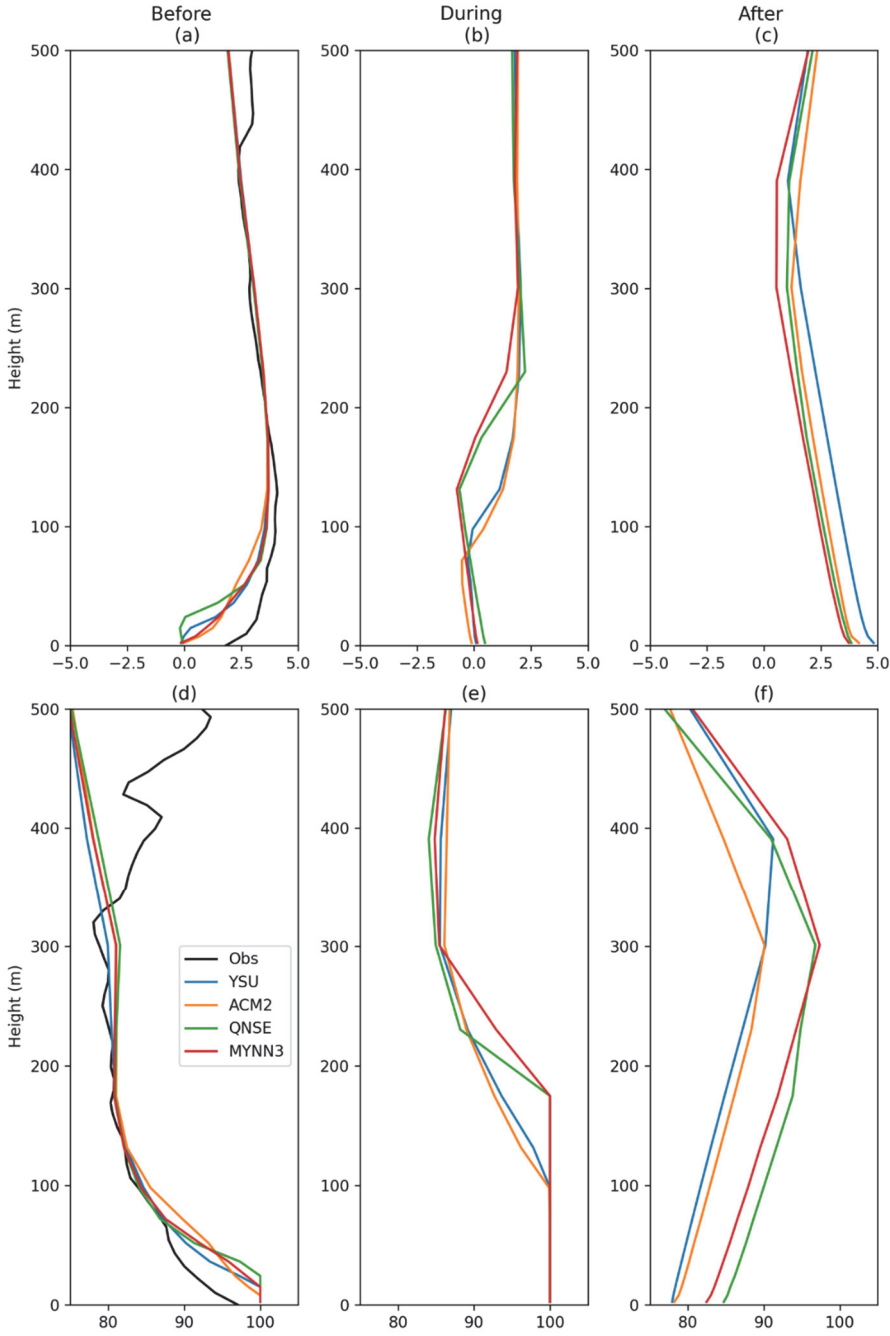


Fig. 8. Vertical profile of temperature and relative humidity before (a, d), during (b, e), and after (c, f) the over Szeged.

Fig. 8 shows the vertical profile of temperature and RH in three phases of the fog evolution such as before fog onset (November 24, 2020, 00:00 UTC), during the fog (November 24, 2020 06:00 UTC) and after the fog (November 24, 2020, 10:30 UTC) at a grid point near Szeged. In *Fig. 8a, 8d*, the calculated vertical profiles of temperature and RH are compared with sounding profiles. (The observed profiles are plotted only in *Fig. 8a, and 8d*, because sounding data are available only at 00:00 UTC). The numerical simulation underestimates the temperature in the layer of 0 – ~200 m. While YSU and MYNN3 PBL schemes, similarly to the observed profile, result in strong inversion below 100 m from surface, ACM2 and QNSE PBL schemes perform inversion layer started above the surface. The RH is overestimated in each case in a very shallow layer of about 50 m. The observation error can be significant when the atmosphere is near the saturation.

The applied PBL parameterization technique significantly impacts the vertical profiles during and after the fog. The nonlocal schemes (YSU and ACM2) result in shallower fog layer than the local schemes (QNSE and MYNN3). The layer characterized by 100% RH and altitude of the inversion layer is deeper in the case of the local PBL schemes than in the case of the nonlocal schemes (*Fig. 8b and 8e*). The altitude of the inversion layer should coincide approximately with the top of the fog. The plots about RH also support the above statements. During the fog event, the atmosphere is saturated near the surface, and the depth of the saturated layer correspond, to the altitude of inversion layer (*Fig. 8e and 8b*). The difference between the local and nonlocal schemes are more conspicuous if the RH profiles are compared in *Fig. 8f*.

3.2. Liquid water content (LWC)

The processes occur in PBL affect not only the dynamics and thermodynamics of the atmosphere, but also impact the fog microphysics. The most important characteristic of the fog is the amount of the condensed vapor that is the liquid water content (hereafter LWC). In this section the results about the sensitivity of the amount of LWC on the applied PBL schemes are presented. The objective is to determine which PBL scheme is able to simulate more accurately the characteristics (e.g., duration, visibility) of the fog.

Fig. 9 and Fig. 10 show the PBL sensitivity results of simulated time series of the vertical profile of LWC at the grid points near the location of the observation at Pécs and Szeged. These plots clearly correspond to the back scatter data (*Fig. 2*). Over Pécs, both the observation and the numerical simulation exclude the fog formation during morning on November 24. At the location of Szeged, the WRF simulations with each PBL scheme produce fog during the early morning on November 24. The simulated onset time of the fog is not accurate comparing with the ceilometer data, and all the PBL schemes produced early fog onset at the first level of the model (*Fig. 3 and Fig. 10*). YSU and ACM2 schemes

produced less amount of LWC at fog onset (04:30 UTC). QNSE and MYNN3 schemes produced significantly high amount of LWC at fog onset (04:30 UTC), and it is corresponding to low visibility (*Fig. 3*). However, numerical models forecast significantly earlier dissipation of the fog. The different PBL schemes result in fog with different lifetimes, LWCs, and thicknesses. YSU and ACM2 schemes simulate significantly smaller LWC compared to QNSE and MYNN3 schemes. The faster dissipation of the fog in the case of YSU and ACM2 schemes can be explained by the fact, that these schemes are characterized by producing warmer and drier daytime in the PBL (*Cohen et al., 2015*). QNSE scheme seems to overestimate both the LWC and the duration of the fog, as it depicts too cool, moist shallow PBL for simulations (*Cohen et al., 2015; Sukoriansky et al., 2005*). Our results support the results published by *Nakanishi and Niino (2006)*, that MYNN3 PBL scheme reasonably depicts the formation of the statically stable boundary layer, which contributes to the reliable simulations of radiation fog. The LWC are integrated for the entire model domain (below 1000 m height) to analyze the impact of the different PBL schemes on the drop formation. *Fig. 11* shows the histograms about the frequency of the LWC for different ranges of mixing ratios at the simulation time of November 24, 2020, 06:00 UTC. The height of the columns means the integrated LWC over the domain at each range of the mixing ratio. The most evident characteristics of the histograms that the QNSE scheme produces significantly larger amount of LWC in the last three ranges than the three other PBL schemes, and the MYNN3 scheme results in more liquid drops at the smaller ranges and less liquid in the larger ranges.

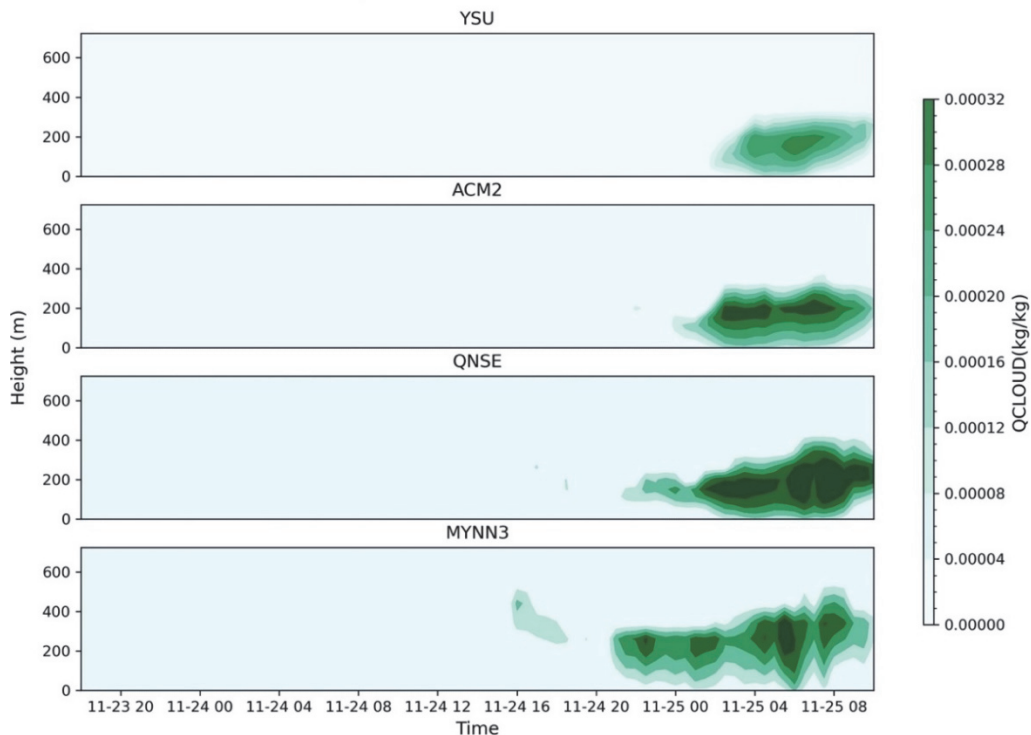


Fig. 9. Time series of the vertical profile of LWC over Péc in case of the four different PBL schemes. Time is depicted as month-day hour (in CET).

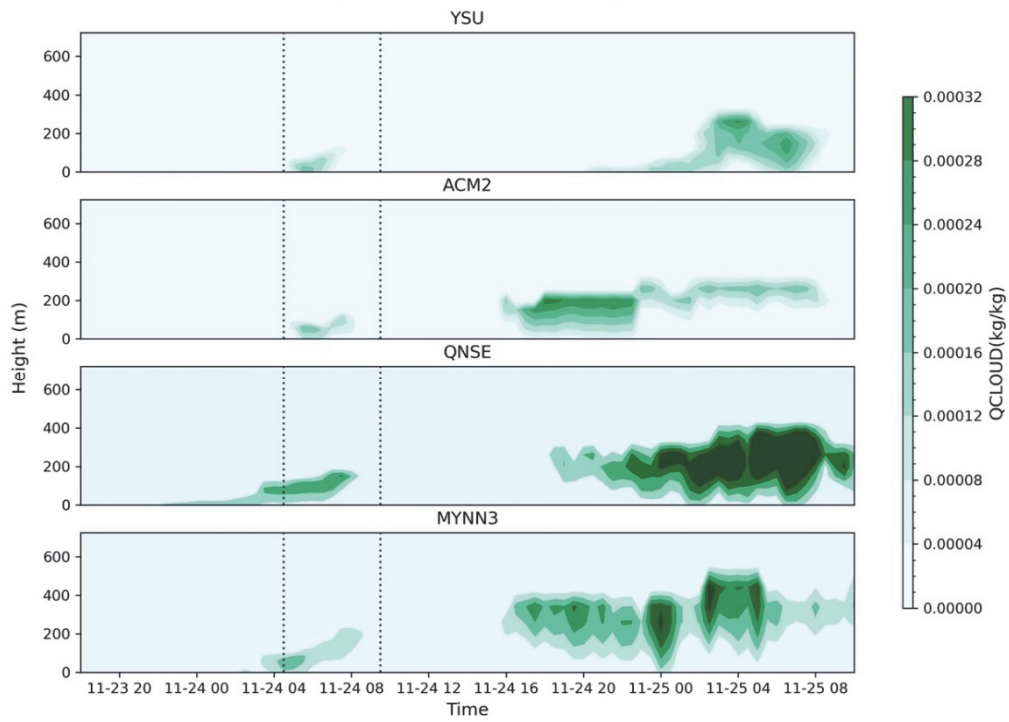


Fig. 10. Time series of the vertical profile of LWC over Szeged in the case of the four different PBL schemes. Time is depicted as month-day hour (in CET).

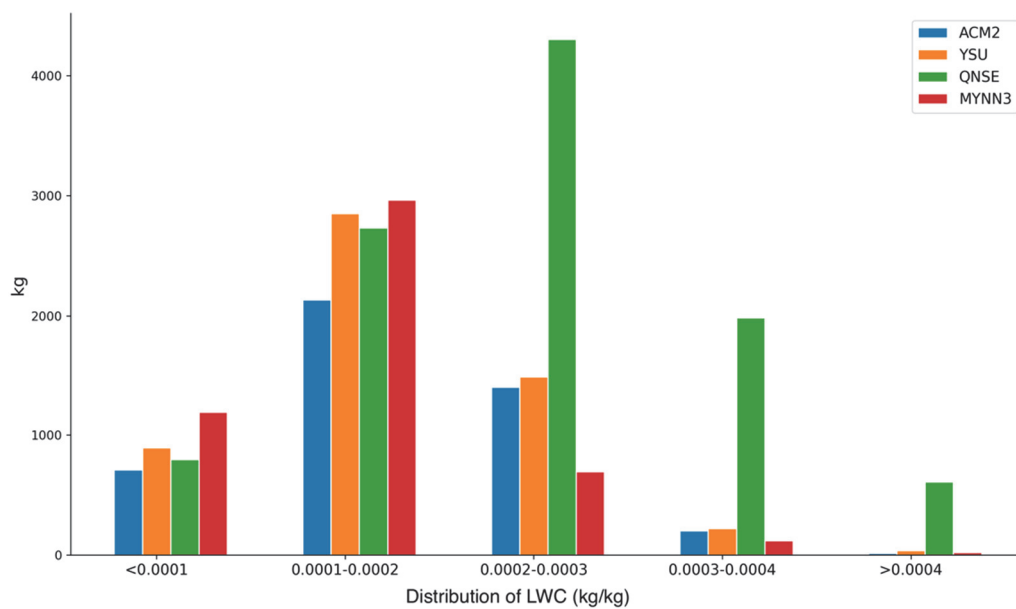


Fig. 11. Histograms of the domain integrated LWC at different ranges at the simulation time of November 24, 2020, 06:00 UTC (approximately at the middle of the fog period).

Fig12 shows the spatial distribution of LWC at the first level of the model in the case of the different PBL schemes at November 24, 2020, 06:00 UTC. All the schemes produced LWC over a relatively large area in the eastern and northwestern parts of Hungary. The numerical simulation using MYNN3 PBL scheme gives the best agreement with the satellite observation (*Fig. 1*). While QNSE scheme produces large values of LWC and overestimate the horizontal extension of the fog, the YSU and ACM2 schemes underestimate the horizontal extension of the fog near the southern border of Hungary.

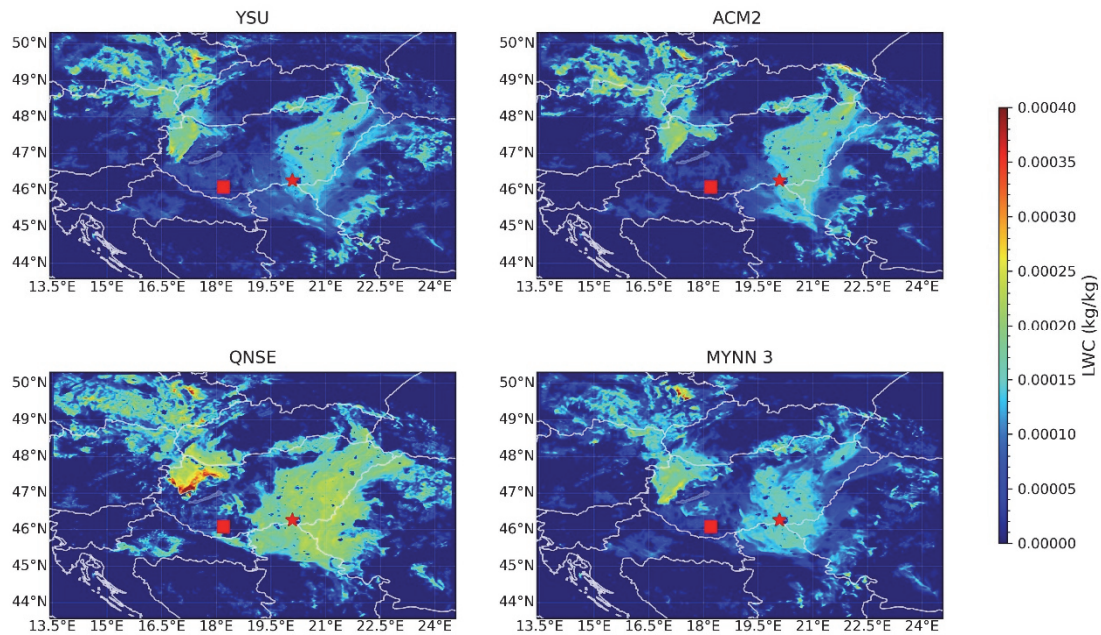


Fig. 12. Spatial distribution of LWC at November 24, 2020 06:00 UTC at the altitude of 6 m.

3.3. Visibility calculation

The forecast of the visibility is one of the largest challenges for meteorologists. As it was presented above, the LWC is impacted not only by the cloud microphysics, but the accurate simulation of PBL processes is also required. Even more, although the impact of the soil or that of the radiation has not been studied in this research, they also play important role in the fog evolution. Another issue is that the visibility can be evaluated accurately if the size distribution of the drops in the fog is available. Unfortunately, the implementation of a bin microphysical scheme in the operational weather forecast numerical model is not an option. So, a parameterized formula should be applied to estimate the visibility. Two-moment bulk microphysical schemes, which predict both the number concentration of liquid drops and LWC, allow a more sophisticated evaluation of

the visibility than the one-moment schemes (they forecast only the LWC). *Gultepe et al.* (2006) asserted that the evaluation of visibility without taking into consideration of the variability in drop concentration could cause 50% uncertainty in the estimation of the visibility. In this study we calculate visibility by substituting the forecasted LWC and drop concentration in the equation as follows (*Song et al.*, 2019):

$$Vis = \frac{0.511}{(LWC \times N_d)^{0.52}}, \quad (1)$$

where N_d is the drop concentration. *Fig. 13* shows the calculated ground (first model) level spatial visibility at November 24, 2020, 06:00 UTC. It has to be noticed, that the spatial distribution is corresponded with the satellite image.

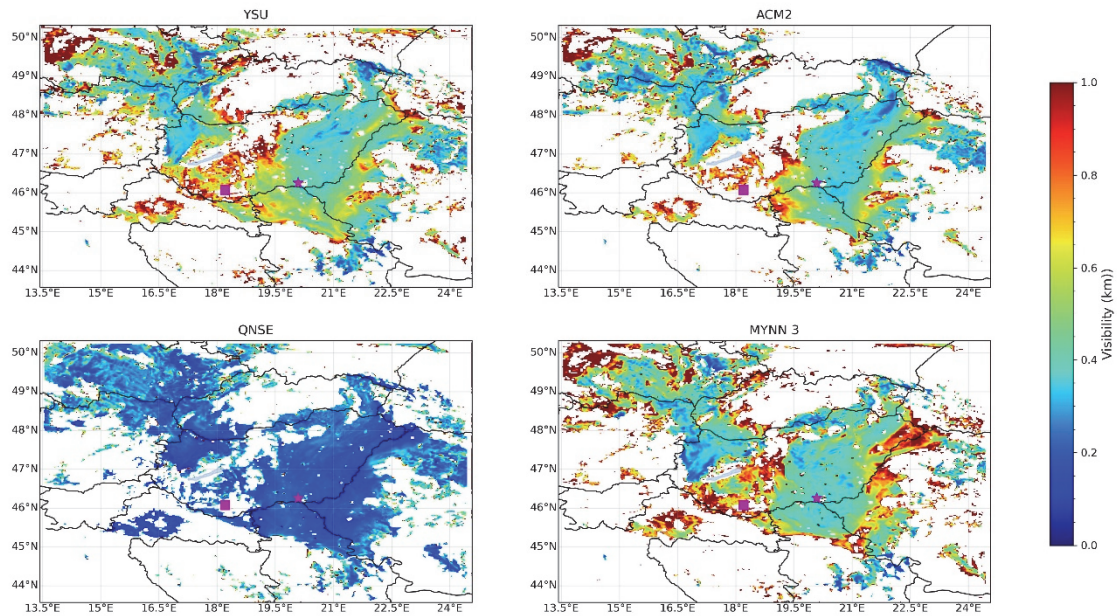


Fig. 13. Spatial distribution of visibility over 6 m height (first model level) at November 24, 2020. 06:00 UTC.

Fig. 3 shows the time evolution of the observed and simulated visibility. All PBL schemes results in early onset of fog (*Fig. 3*), even more, QNSE scheme produced visibility less than 200 m at model fog onset and started to increase the visibility at fog onset observed. Both nonlocal schemes (YSU and ACM2) produced visibility greater than 500 m at model fog onset which started to decrease significantly after fog onset observed. Among all PBL schemes MYNN3 results in significant decrease of visibility slightly before the observed fog onset

(04:30 UTC) and maintained low visibility until the hours of the fog, resulting in earlier dissipation comparing with other observations (*Fig. 3*).

4. Discussion and conclusion

The main aim of this study was to better understand the capability of the WRF model to simulate the fog lifecycle for an extremely fog event that occurred in the time period of 04:30 UTC - 09:30 UTC on November 24, 2020. Detailed PBL sensitivity experiments have been accomplished by using numerical mesoscale model (WRF) to understand the model ability for fog prediction. A novel microphysical module, the GOCART–Thompson scheme, was implemented into WRF-ARW to couple the GOCART aerosol model to the aerosol-aware Thompson–Eidhammer microphysics scheme (*Thompson and Eidhammer, 2014*). The results of four different PBL schemes have been compared. These schemes involve different parameterizations for the turbulence which contributes to the mixing of heat and moisture. The model data are compared with observational data such as surface temperature, backscatter data from ceilometer measured at two locations, Pécs and Szeged, furthermore, with radio sounding data at Szeged. In agreement with the observations the numerical models, independently off the applied PBL schemes, provide fog at Szeged, do not provide fog at Pécs. Strong impact of the boundary layer processes on fog microphysics is proved by comparing the LWC calculated by using different PBL schemes. Unfortunately, observation data on the LWC is not available for this fog event. So, comparison of the satellite observations and the visibility data (it depends on both the drop concentration and LWC) with the model results, allows us to validate the simulated values. The QNSE results in unrealistic such as early fog formation, high amount of LWC and underestimated visibility at fog onset. The numerical models are not able to forecast the duration (too early onset and early dissipation) of the fog, independently which PBL schemes are used (*Fig. 4g*). *Fig. 4g* shows that all the PBL schemes are simulated early onset fog over Szeged, and indicates that no particular scheme is suitable fog forecasting. Based on our simulations, previous publications (*Pithani et al., 2019b, 2018b; Smith et al., 2021*) and the calculated characteristics, the MYNN3 scheme is suggested to use for the numerical forecast of the fog.

Thermodynamics and dynamics occur in PBL play fundamental role in fog formation. In this research, a sensitivity test was accomplished to study how the parameterization of PBL processes impact the accuracy of fog forecast.

The conclusions of the PBL sensitivity experiment are as follows:

- The parameterization of the PBL schemes significantly impacts the fog microphysics, especially the amount of LWC. While the QNSE scheme results in unrealistic early formation of the fog (and too large LWC), the

duration of the fog is rather short if the nonlocal schemes (YSU and ACM2) are applied. Although even the MYNN3 scheme results in too early dissipation of the fog, the results suggest that the MYNN3 scheme is well suitable for fog prediction over Hungary.

- Unfortunately, all the simulation results (independently of the applied PBL scheme) show, that the dissipation of the fog starts too early (*Pithani et al.*, 2019c, 2018b). The reason of this is not known. Because not only PBL processes, but the interaction between the atmosphere and the soil, and the effect of the radiation can be also decisive, further research is required to solve this problem.

References

- Benjamin, S.G., Dévényi, D., Weygandt, S.S., Brundage, K.J., Brown, J.M., Grell, J.A., Kim, D., Schwartz, B.E., Smirnova, T.G., Smith, T.L., and Manikin, G.S.*, 2004: An hourly assimilation/forecast cycle: the RUC model. *Mon. Weather Rev.* 132, 495–518. [https://doi.org/10.1175/1520-0493\(2004\)132<0495:AHACTR>2.0.CO;2](https://doi.org/10.1175/1520-0493(2004)132<0495:AHACTR>2.0.CO;2)
- Benoit, R., Desgagné, M., Pellerin, P., Pellerin, S., Chartier, Y., and Desjardins, S.*, 1997: The Canadian MC2: A semi-Lagrangian, semi-implicit wideband atmospheric model suited for finescale process studies and simulation. *Mon. Weather Rev.* 125, 2382–2415. [https://doi.org/10.1175/1520-0493\(1997\)125<2382:TCMASL>2.0.CO;2](https://doi.org/10.1175/1520-0493(1997)125<2382:TCMASL>2.0.CO;2)
- Chaouch, N., Temimi, M., Weston, M., and Ghedira, H.*, 2017: Sensitivity of the meteorological model WRF-ARW to planetary boundary layer schemes during fog conditions in a coastal arid region. *Atmos. Res.* 187, 106–127. <https://doi.org/10.1016/j.atmosres.2016.12.009>
- Chen, C., Zhang, M., Perrie, W., Chang, R., Chen, X., Duplessis, P., and Wheeler, M.*, 2020: Boundary Layer Parameterizations to Simulate Fog Over Atlantic Canada Waters. *Earth Space Sci.* 7. e2019EA000703. <https://doi.org/10.1029/2019EA000703>
- Chen, F. and Dudhia, J.*, 2001: Coupling an advanced land surface–hydrology model with the Penn State–NCAR MM5 modeling system. Part I: Model implementation and sensitivity. *Mon. Weather Rev.* 129, 569–585. [https://doi.org/10.1175/1520-0493\(2001\)129<0569:CAALSH>2.0.CO;2](https://doi.org/10.1175/1520-0493(2001)129<0569:CAALSH>2.0.CO;2)
- Chin, M., Ginoux, P., Kinne, S., Torres, O., Holben, B.N., Duncan, B.N., Martin, R. v., Logan, J.A., Higurashi, A., and Nakajima, T.*, 2002: Tropospheric aerosol optical thickness from the GOCART model and comparisons with satellite and sun photometer measurements. *J. Atmos. Sci.* 59, 461–483. [https://doi.org/10.1175/1520-0469\(2002\)059<0461:TAOTFT>2.0.CO;2](https://doi.org/10.1175/1520-0469(2002)059<0461:TAOTFT>2.0.CO;2)
- Cohen, A.E., Cavallo, S.M., Coniglio, M.C., and Brooks, H.E.*, 2015: A review of planetary boundary layer parameterization schemes and their sensitivity in simulating southeastern U.S. cold season severe weather environments. *Weather Forecast.* 30, 591–612. <https://doi.org/10.1175/WAF-D-14-00105.1>
- Coniglio, M.C.*, 2012: Verification of RUC 0-1-h forecasts and SPC mesoscale analyses using VORTEX2 soundings. *Weather Forecast.* 27, 667–683. <https://doi.org/10.1175/WAF-D-11-00096.1>
- Cséplő, A., Sarkadi, N., Horváth, Á., Schmeller, G., and Lemler, T.*, 2019. Fog climatology in Hungary. *Időjárás* 123, 241–264. <https://doi.org/10.28974/idojaras.2019.2.7>
- Fuzzi, S., Laj, P., Ricci, L., Orsi, G., Heintzenberg, J., Wendisch, M., Yuskiewicz, B., Mertes, S., Orsini, D., Schwanz, M., Wiedensohler, A., Stratmann, F., Berg, O.H., Swietlicki, E., Frank, G., Martinsson, B.G., Günther, A., Dierssen, J.P., Schell, D., Jaeschke, W., Berner, A., Dusek, U., Galambos, Z., Kruisz, C., Mesfin, N.S., Wobrock, W., Arends, B., Brink, and H. ten*, 1998: Overview of the Po valley fog experiment 1994 (CHEMDROP). *Contr. Atmos. Phys.* 71, 3–19.

- García-Díez, M., Fernández, J., Fita, L., and Yagüe, C., 2013: Seasonal dependence of WRF model biases and sensitivity to PBL schemes over Europe. *Quart. J. Roy. Meteorol. Soc.* 139, 501–514. <https://doi.org/10.1002/qj.1976>
- Geresd, I., Xue, L., Sarkadi, N., and Rasmussen, R., 2020: Evaluation of orographic cloud seeding using a bin microphysics scheme: Three-dimensional simulation of real cases. *J. Appl. Meteorol. Climatol.* 59, 1537–1555. <https://doi.org/10.1175/JAMC-D-19-0278.1>
- Ghude, S.D., Bhat, G.S., Prabhakaran, T., Jenamani, R.K., Chate, D.M., Safai, P.D., Karipot, A.K., Konwar, M., Pithani, P., Sinha, V., Rao, P.S.P., Dixit, S.A., Tiwari, S., Todekar, K., Varpe, S., Srivastava, A.K., Bisht, D.S., Murugavel, P., Ali, K., Mina, U., Dharua, M., Jaya Rao, Y., Padmakumari, B., Hazra, A., Nigam, N., Shende, U., Lal, D.M., Chandra, B.P., Mishra, A.K., Kumar, A., Hakkim, H., Pawar, H., Acharja, P., Kulkarni, R., Subharthi, C., Balaji, B., Varghese, M., Bera, S., and Rajeevan, M., 2017: Winter fog experiment over the Indo-Gangetic plains of India. *Curr. Sci.* 112, 767–784. <https://doi.org/10.18520/cs/v112/i04/767-784>
- Ginoux, P., Chin, M., Tegen, I., Goddard, T., In- G., 2001. model Brent Holben •’ Oleg Dubovik •,•’ and Shian-Jiann Lin e CART) model . In this model all topographic from the Goddard Earth Observing System Data Assimilation System (GEOS emission is estimated to be between. 2-Journal of Geophysical Research 106, 20255–20273.
- Gultepe, I., 2019: Low-Level Ice Clouds-Ice Fog. Encyclopedia of Water: Science, Technology, and Society 1–19. <https://doi.org/10.1002/9781119300762.wsts0140>
- Gultepe, I., 2007: Fog and Boundary Layer Clouds: Fog Visibility and Forecasting, Fog and Boundary Layer Clouds: Fog Visibil. Forecast. <https://doi.org/10.1007/978-3-7643-8419-7>
- Gultepe, I., Müller, M.D., and Boybeyi, Z., 2006: A new visibility parameterization for warm-fog applications in numerical weather prediction models. *J. Appl. Meteorol. Climatol.* 45, 1469–1480. <https://doi.org/10.1175/JAM2423.1>
- Gultepe, I., Tardif, R., Michaelides, S.C., Cermak, J., Bott, A., Bendix, J., Müller, M.D., Pagowski, M., Hansen, B., Ellrod, G., Jacobs, W., Toth, G., and Cober, S.G., 2007: Fog research: A review of past achievements and future perspectives. *Pure Appl. Geophys.* 164, 1121–1159. <https://doi.org/10.1007/s00024-007-0211-x>
- Haeffelin, M., Bergot, T., Elias, T., Tardif, R., Carrer, D., Chazette, P., Colomb, M., Drobinski, P., Dupont, E., Dupont, J.C., Gomes, L., Musson-Genon, L., Pietras, C., Plana-Fattori, A., Protat, A., Rangognio, J., Raut, J.C., Rémy, S., Richard, D., Sciare, J., and Zhang, X., 2010: PARISFOG: Shedding new light on fog physical processes. *Bull. Amer. Meteorol. Soc.* 91, 767–783. <https://doi.org/10.1175/2009BAMS2671.1>
- Hong, S.Y., Noh, Y., and Dudhia, J., 2006: A new vertical diffusion package with an explicit treatment of entrainment processes. *Mon. Weather Rev.* 134, 2318–2341. <https://doi.org/10.1175/MWR3199.1>
- Horváth, A., Geresdi, I., Németh, P., Csirmaz, K., and Dombai, F., 2009: Numerical modeling of severe convective storms occurring in the Carpathian Basin. *Atmos. Res.* 93, 221–237. <https://doi.org/10.1016/j.atmosres.2008.10.019>
- Horváth Á., Geresdi I., Németh P., and Dombai F., 2007: The Constitution Day storm in Budapest: Case study of the August 20, 2006 severe storm. *Időjárás* 111, 41–63.
- Hu, X.M., Nielsen-Gammon, J.W., and Zhang, F., 2010. Evaluation of three planetary boundary layer schemes in the WRF model. *J. Appl. Meteorol. Climatol.* 49, 1831–1844. <https://doi.org/10.1175/2010JAMC2432.1>
- Iacono, M.J., Delamere, J.S., Mlawer, E.J., Shephard, M.W., Clough, S.A., and Collins, W.D., 2008: Radiative forcing by long-lived greenhouse gases: Calculations with the AER radiative transfer models. *J. Geophys Res: Atmos* 113. D13103. <https://doi.org/10.1029/2008JD009944>
- Lábó, E. and Geresdi, I., 2016: Study of longwave radiative transfer in stratocumulus clouds by using bin optical properties and bin microphysics scheme. *Atmos. Res.* 167, 61–76. <https://doi.org/10.1016/j.atmosres.2015.07.016>
- Mihailovic, D.T., 2006: Impact of local and non-local eddy-diffusivity schemes on calculating the concentration of pollutants in environmental models. Proceedings of the iEMSs 3rd Biennial Meeting, "Summit on Environmental Modelling and Software".

- Nakanishi, M. and Niino, H., 2006: An improved Mellor-Yamada Level-3 model: Its numerical stability and application to a regional prediction of advection fog. *Bound.-Lay. Meteorol.* 119, 397–407. <https://doi.org/10.1007/s10546-005-9030-8>
- Pithani, P., Ghude, S.D., Chennu, V.N., Kulkarni, R.G., Steeneveld, G.J., Sharma, A., Prabhakaran, T., Chate, D.M., Gultepe, I., Jenamani, R.K., and Madhavan, R., 2019a: WRF Model Prediction of a Dense Fog Event Occurred During the Winter Fog Experiment (WIFEX). *Pure Appl. Geophys.* 176, 1827–1846. <https://doi.org/10.1007/s00024-018-2053-0>
- Pithani, P., Ghude, S.D., Chennu, V.N., Kulkarni, R.G., Steeneveld, G.J., Sharma, A., Prabhakaran, T., Chate, D.M., Gultepe, I., Jenamani, R.K., and Madhavan, R., 2019b: WRF Model Prediction of a Dense Fog Event Occurred During the Winter Fog Experiment (WIFEX). *Pure Appl. Geophys.* 176, 1827–1846. <https://doi.org/10.1007/s00024-018-2053-0>
- Pithani, P., Ghude, S.D., Chennu, V.N., Kulkarni, R.G., Steeneveld, G.J., Sharma, A., Prabhakaran, T., Chate, D.M., Gultepe, I., Jenamani, R.K., and Madhavan, R., 2019c: WRF Model Prediction of a Dense Fog Event Occurred During the Winter Fog Experiment (WIFEX). *Pure Appl. Geophys.* 176, 1827–1846. <https://doi.org/10.1007/s00024-018-2053-0>
- Pithani, P., Ghude, S.D., Prabhakaran, T., Karipot, A., Hazra, A., Kulkarni, R., Chowdhuri, S., Resmi, E.A., Konwar, M., Murugavel, P., Safai, P.D., Chate, D.M., Tiwari, Y., Jenamani, R.K., and Rajeevan, M., 2018a. WRF model sensitivity to choice of PBL and microphysics parameterization for an advection fog event at Barkachha, rural site in the Indo-Gangetic basin, India. *Theor. Appl. Climatol.* 136, 1199–1113. <https://doi.org/10.1007/s00704-018-2530-5>
- Pithani, P., Ghude, S.D., Prabhakaran, T., Karipot, A., Hazra, A., Kulkarni, R., Chowdhuri, S., Resmi, E.A., Konwar, M., Murugavel, P., Safai, P.D., Chate, D.M., Tiwari, Y., Jenamani, R.K., and Rajeevan, M., 2018b. WRF model sensitivity to choice of PBL and microphysics parameterization for an advection fog event at Barkachha, rural site in the Indo-Gangetic basin, India. *Theoretical and Applied Climatology* 1–15. <https://doi.org/10.1007/s00704-018-2530-5>
- Pleim, J.E., 2007: A combined local and nonlocal closure model for the atmospheric boundary layer. Part I: Model description and testing. *J. Appl. Meteorol. Climatol.* 46, 1383–1395. <https://doi.org/10.1175/JAM2539.1>
- Pleim, J.E., 2007: A combined local and nonlocal closure model for the atmospheric boundary layer. Part II: Application and evaluation in a mesoscale meteorological model. *J. Appl. Meteorol. Climatol.* 46, 1396–1409. <https://doi.org/10.1175/JAM2534.1>
- Rockel, B., Will, A., and Hense, A., 2008: The regional climate model COSMO-CLM (CCLM). *Meteorol. Zeit.* 17, 347–348. <https://doi.org/10.1127/0941-2948/2008/0309>
- Saito, K., Fujita, T., Yamada, Y., Ishida, J.I., Kumagai, Y., Aranami, K., Ohmori, S., Nagasawa, R., Kumagai, S., Muroi, C., Kato, T., Eito, H., and Yamazaki, Y., 2006. The operational JMA nonhydrostatic mesoscale model. *Mon. Weather Rev.* 134, 1266–1298. <https://doi.org/10.1175/MWR3120.1>
- Sarkadi, N., Geresdi, I., and Thompson, G., 2016. Numerical simulation of precipitation formation in the case orographically induced convective cloud: Comparison of the results of bin and bulk microphysical schemes. *Atmos. Res.* 180, 241–261. <https://doi.org/10.1016/j.atmosres.2016.04.010>
- Skamarock, W.C., Klemp, J.B., Dudhia, J.B., Gill, D.O., Barker, D.M., Duda, M.G., Huang, X.-Y., Wang, W., and Powers, J.G., 2008: A description of the Advanced Research WRF Version 3, NCAR Technical Note TN-475+STR. Technical Report 113.
- Smith, D.K.E., Renfrew, I.A., Dorling, S.R., Price, J.D., and Boutle, I.A., 2021: Sub-km scale numerical weather prediction model simulations of radiation fog. *Quart. J. Roy. Meteorol. Soc.* 147, 746–763. <https://doi.org/10.1002/qj.3943>
- Song, J.I., Yum, S.S., Gultepe, I., Chang, K.H., and Kim, B.G., 2019: Development of a new visibility parameterization based on the measurement of fog microphysics at a mountain site in Korea. *Atmos. Res.* 229, 115–126. <https://doi.org/10.1016/j.atmosres.2019.06.011>
- Sukoriansky, S., Galperin, B., and Perov, V., 2005: Application of a new spectral theory of stably stratified turbulence to the atmospheric boundary layer over sea ice. *Bound.-Lay. Meteorol.* 117, 231–257. <https://doi.org/10.1007/s10546-004-6848-4>

- Thériault, J.M., Milbrandt, J.A., Doyle, J., Minder, J.R., Thompson, G., Sarkadi, N., and Geresdi, I., 2015. Impact of melting snow on the valley flow field and precipitation phase transition. Atmos. Res. 156, 111–124. <https://doi.org/10.1016/j.atmosres.2014.12.006>*
- Thompson, G. and Eidhammer, T., 2014a: A Study of Aerosol Impacts on Clouds and Precipitation Development in a Large Winter Cyclone. J. Atmos. Sci. 71, 3636–3658. <https://doi.org/10.1175/JAS-D-13-0305.1>*
- Thompson, G. and Eidhammer, T., 2014b: A study of aerosol impacts on clouds and precipitation development in a large winter cyclone. J. Atmos. Sci. 71, 3636–3658. <https://doi.org/10.1175/JAS-D-13-0305.1>*
- Twomey, S., 1984: Pollution and the Planetary Albedo. Atmos. Environ. 41, 120–125. <https://doi.org/10.1016/j.atmosenv.2007.10.062>*